# NAVAL POSTGRADUATE SCHOOL

## MONTEREY, CALIFORNIA

# THESIS

**ENHANCING SPACE SITUATIONAL AWARENESS USING A 3U CUBESAT WITH OPTICAL IMAGER**

by

Jason A. Flanagan

December 2010

| | |
|---|---|
| Thesis Advisor: | James H. Newman |
| Second Reader: | Marcello Romano |

**Approved for public release; distribution is unlimited**

THIS PAGE INTENTIONALLY LEFT BLANK

| REPORT DOCUMENTATION PAGE | | *Form Approved OMB No. 0704-0188* |
|---|---|---|
| Public reporting burden for this collection of information is estimated to average 1 hour per response, including the time for reviewing instruction, searching existing data sources, gathering and maintaining the data needed, and completing and reviewing the collection of information. Send comments regarding this burden estimate or any other aspect of this collection of information, including suggestions for reducing this burden, to Washington headquarters Services, Directorate for Information Operations and Reports, 1215 Jefferson Davis Highway, Suite 1204, Arlington, VA 22202-4302, and to the Office of Management and Budget, Paperwork Reduction Project (0704-0188) Washington DC 20503. | | |
| **1. AGENCY USE ONLY** *(Leave blank)* | **2. REPORT DATE** December 2010 | **3. REPORT TYPE AND DATES COVERED** Master's Thesis |
| **4. TITLE AND SUBTITLE** Enhancing Space Situational Awareness using a 3U CubeSat with Optical Imager | | **5. FUNDING NUMBERS** |
| **6. AUTHOR(S)** Flanagan, Jason A. | | |
| **7. PERFORMING ORGANIZATION NAME(S) AND ADDRESS(ES)** Naval Postgraduate School Monterey, CA 93943-5000 | | **8. PERFORMING ORGANIZATION REPORT NUMBER** |
| **9. SPONSORING /MONITORING AGENCY NAME(S) AND ADDRESS(ES)** N/A | | **10. SPONSORING/MONITORING AGENCY REPORT NUMBER** |
| **11. SUPPLEMENTARY NOTES** The views expressed in this thesis are those of the author and do not reflect the official policy or position of the Department of Defense or the U.S. Government. IRB Protocol number _____. | | |
| **12a. DISTRIBUTION / AVAILABILITY STATEMENT** Approved for public release; distribution is unlimited | | **12b. DISTRIBUTION CODE** |
| **13. ABSTRACT (maximum 200 words)** Space situational awareness is extremely important in order to maintain the safety and usability of earth-orbiting satellites, as well as protecting astronauts living and working in space. Traditional space situational awareness is achieved using ground-based radar and optical sensors. This thesis explores the feasibility of space-based space situational awareness using a 3U CubeSat with an optical imager to augment the Space Surveillance Network by capturing conjunctions in space, from which ephemeris data of earth orbiting objects can be updated to more accurately predict future orbital positions. Work completed includes preliminary work towards building, testing, and using a Colony II Bus emulator and interface mechanism, allowing smooth payload and bus integration. Analysis of orbital trajectories for a reference orbit and potential crossing satellites provides insight into the capabilities of the SSA CubeSat. Future work is discussed. | | |
| **14. SUBJECT TERMS** 3U, CubeSat, Space Situational Awareness, Space Surveillance Network, Colony II Bus, Boeing, Optical Imager, Ephemeris, Conjunction | | **15. NUMBER OF PAGES** 71 |
| | | **16. PRICE CODE** |
| **17. SECURITY CLASSIFICATION OF REPORT** Unclassified | **18. SECURITY CLASSIFICATION OF THIS PAGE** Unclassified | **19. SECURITY CLASSIFICATION OF ABSTRACT** Unclassified | **20. LIMITATION OF ABSTRACT** UU |

NSN 7540-01-280-5500

Standard Form 298 (Rev. 2-89)
Prescribed by ANSI Std. 239-18

i

THIS PAGE INTENTIONALLY LEFT BLANK

**ENHANCING SPACE SITUATIONAL AWARENESS USING A 3U CUBESAT WITH OPTICAL IMAGER**

Jason A. Flanagan
Lieutenant, United States Navy
B.S., North Carolina State University, 2004

Submitted in partial fulfillment of the
requirements for the degree of

**MASTER OF SCIENCE IN ASTRONAUTICAL ENGINEERING**

from the

**NAVAL POSTGRADUATE SCHOOL
December 2010**

Author:            Jason Flanagan

Approved by:     James H. Newman
                    Thesis Advisor

                    Marcello Romano
                    Second Reader

                    Knox T. Millsaps
                    Chairman, Department of Mechanical and Astronautical Engineering

THIS PAGE INTENTIONALLY LEFT BLANK

# ABSTRACT

Space situational awareness is extremely important in order to maintain the safety and usability of earth-orbiting satellites, as well as protecting astronauts living and working in space. Traditional space situational awareness is achieved using ground-based radar and optical sensors. This thesis explores the feasibility of space-based space situational awareness using a 3U CubeSat with an optical imager to augment the Space Surveillance Network by capturing conjunctions in space, from which ephemeris data of earth orbiting objects can be updated to more accurately predict future orbital positions. Work completed includes preliminary work towards building, testing, and using a Colony II Bus emulator and interface mechanism, allowing smooth payload and bus integration. Analysis of orbital trajectories for a reference orbit and potential crossing satellites provides insight into the capabilities of the SSA CubeSat. Future work is discussed.

THIS PAGE INTENTIONALLY LEFT BLANK

# TABLE OF CONTENTS

THIS PAGE INTENTIONALLY LEFT BLANK

# LIST OF FIGURES

# LIST OF TABLES

THIS PAGE INTENTIONALLY LEFT BLANK

# LIST OF ACRONYMS AND ABBREVIATIONS

| | |
|---|---|
| 3U | Three Unit CubeSat |
| ASAT | Anti-satellite |
| ASCII | American Standard Code for Information Interchange |
| C2B | Colony II Bus |
| CCD | Charge Coupled Device |
| DAQ | Data Acquisition |
| DIO | Digital Input/Output |
| DLL | Dynamic Link Library |
| EDU | engineering design unit |
| EO | Electro-Optical |
| FY-1C | Fengyun 1C |
| GUI | Graphic User Interface |
| I-board | Interface Board |
| LEO | Low Earth Orbit |
| LLNL | Lawrence Livermore National Laboratory |
| MCC | Measurement Computing Corporation |
| MSX | Midcourse Space Experiment |
| PCB | Printed Circuit Board |
| RSO | Resident Space Object |
| SBSS | Space-Based Space Surveillance |
| SBV | Space-Based Visible |
| SM3 | Standard Missile III |
| SSA | Space Situational Awareness |

SSN          Space Surveillance Network

STARE      Space Telescope for the Actionable Refinement of Ephemeris

STK         Satellite Toolkit

TAMU      Texas A&M University

# ACKNOWLEDGMENTS

I would to thank my wife, Lesley, for her love and support throughout my time at the Naval Postgraduate School. She always had faith in me, and offered the encouragement to keep going, and the patience to endure it right alongside me. This thesis was made possible through the expertise and guidance of Professor James Newman. I would also like to thank Professor Marcello Romano for his assistance along the way. Dan Sakoda, Jim Horning, and David Rigmaiden each played key roles as technical experts with lab equipment, electronics, CAD modeling, and programming. Former students Kevin Smith and Rod Jenkins offered a wealth of knowledge and experience, and were always willing to offer assistance or advice. Lastly, I would like to thank Danny Soria for making sure our class made time to enjoy our time in Monterey.

THIS PAGE INTENTIONALLY LEFT BLANK

# I.     INTRODUCTION

## A.     NAVAL POSTGRADUATE SCHOOL SPACE SITUATIONAL AWARENESS EFFORT

This thesis discusses Space Situational Awareness (SSA), the feasibility of using a CubeSat to enhance space situational awareness, and the steps taken to integrate a CubeSat with an optical imager for that purpose. The author was the first student at the Naval Postgraduate School (NPS) to work on this SSA project. Figure 1 shows an example of a CubeSat with an optical imager for the payload, the Miniature Imaging Spacecraft (MISC) from Pumpkin, Inc.
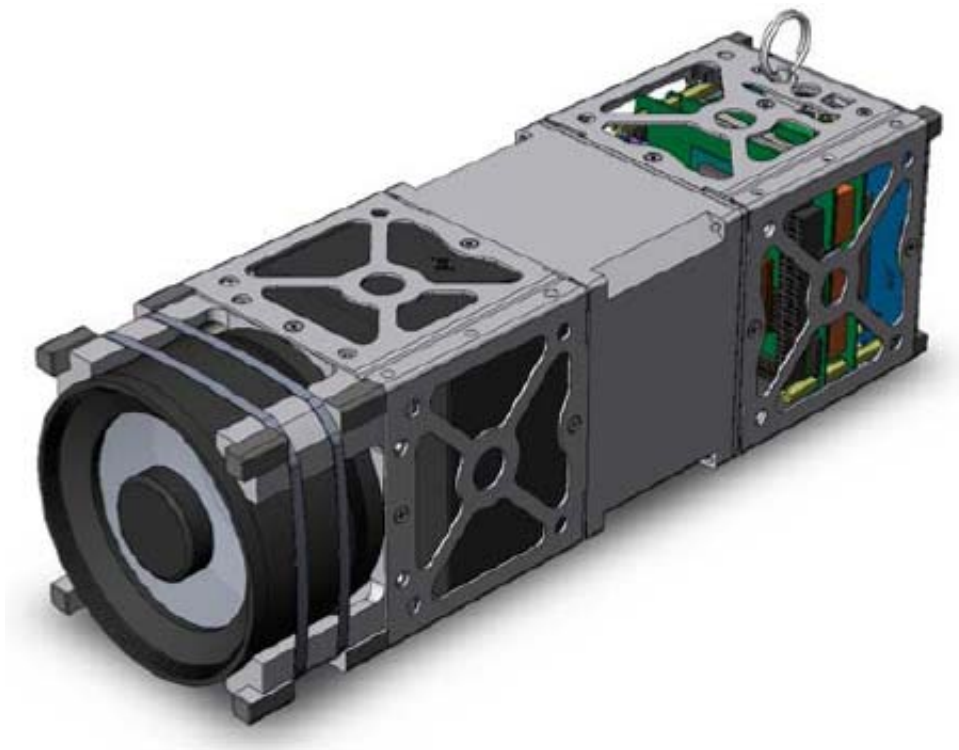


Figure 1.     Miniature Imaging Spacecraft, Pumpkin Inc.(From [1])

In early 2010, Lawrence Livermore National Laboratories (LLNL) proposed a joint SSA project with NPS and Texas A&M University (TAMU). LLNL would develop an optical imager for capturing streaks on a charge coupled device (CCD) camera from

light reflected by satellites in support of the Space Telescope for the Actionable Refinement of Ephemeris (STARE) program. Analysis of these streaks should permit improvement of the orbital ephemeris of the observed satellite. For this project, NPS and TAMU are integrating the payload with the spacecraft bus. The payload is an electro-optical imager, and the spacecraft bus is a Colony II Bus (C2B) from the Boeing Corporation. Since May 2010, LLNL, NPS, and TAMU have participated in telephone conferences to discuss the status of each institution and the work completed, as well as resolving issues that were encountered and deciding the best course of action.

The C2B is a 3U CubeSat. A 1U CubeSat is a very small spacecraft with exterior dimensions of 10cm by 10cm by 10cm. A 2U CubeSat is the size of two CubeSats, with one stacked on the other, with the dimensions of 10cm by 10cm by 20cm. Similarly, a 3U CubeSat, such as the C2B, is the size of three CubeSats stacked, with the dimensions of 10cm by 10cm by 30cm. Figure 2 shows three CubeSats, starting with two 1U on the right, 2U to the left, and 3U on the far left.
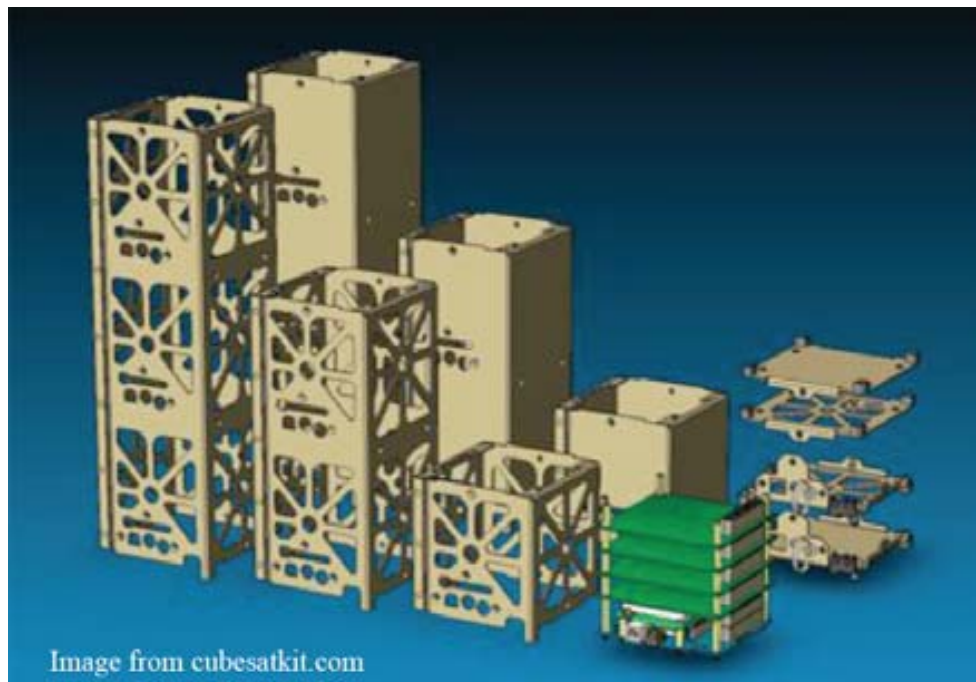


Figure 2.    1U, 2U, and 3U CubeSats (From [1])

## B. SPACE SITUATIONAL AWARENESS

Space situational awareness is the ability to maintain and utilize the knowledge of all Earth orbiting objects, space weather, and radio frequency interference, and how these affect our use of space. Earth orbiting objects include active and inactive satellites, spent rocket bodies, and orbital debris [2]. The United States currently tracks 19,000 man-made objects larger than 10cm, including 800 active satellites. Each of these objects poses a threat to active satellites, with the potential of destroying the satellite and causing even more debris. Figure 3 shows an exaggerated view of the orbiting objects in Low Earth Orbit (LEO). The term space situational awareness was first used by Secretary of Defense Donald Rumsfeld in his 2001 report on space [3].



Figure 3.  Artist rendition of orbital debris in LEO (From [4])

## C. HISTORY

Orbital debris is produced every time a satellite is launched into orbit. Since the first artificial satellite, Sputnik, was launched on October 4, 1957, the amount of debris orbiting the Earth has steadily increased. Every space launch creates orbital debris along with the addition of the active satellite. In addition to routine spacecraft launches,

collisions in space also add to the amount of orbital debris. Just within the past few years, there have been three spacecraft collisions that have brought space situational awareness to the forefront of space related topics.

The first intentional collision in recent history was when a Chinese Fengyun 1C (FY-1C) polar-orbiting weather satellite, shown in Figure 4, was intercepted by a Chinese SC-19 missile on January 11, 2007. The relatively high orbital altitude of the FY-1C, 869km, combined with the high relative velocity between the satellite and missile, created over 3,000 pieces of orbital debris [5]. This impact created a debris field that spans from as low as 200km altitude all the way up to 3,500km. The high altitude debris will take decades to reenter the Earth's atmosphere, causing potential collision for as long as the debris remains in orbit. Figure 5 shows the debris field just five minutes after the collision, where each green dot represents one piece of trackable orbital debris over 10cm. Figure 6 shows the current debris field, where each red dot represents the FY-1C collision debris and each green dot represents all other tracked orbital objects. The green line shows the International Space Station at an altitude of 300km.
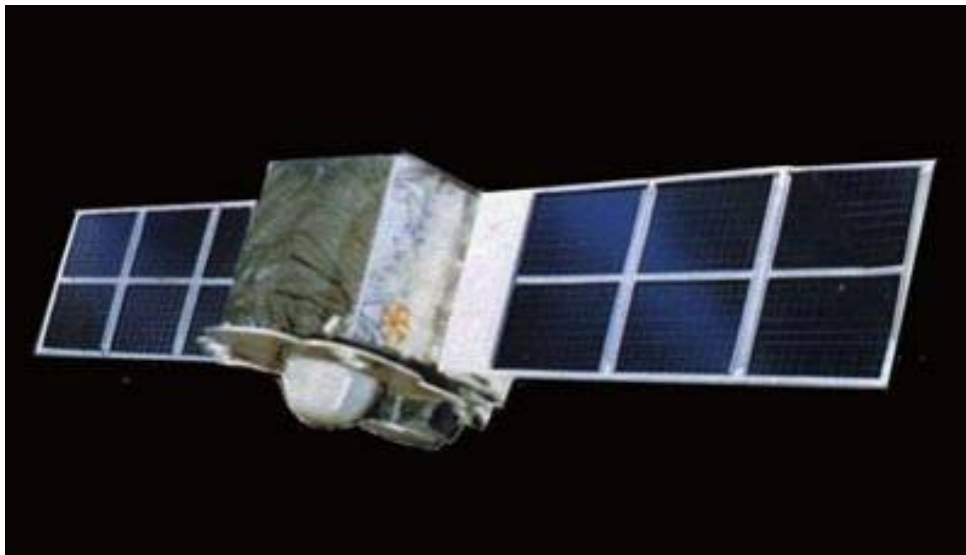


Figure 4.     Chinese FY-1C, intercepted by SC-19, January 11, 2007 (From [5])
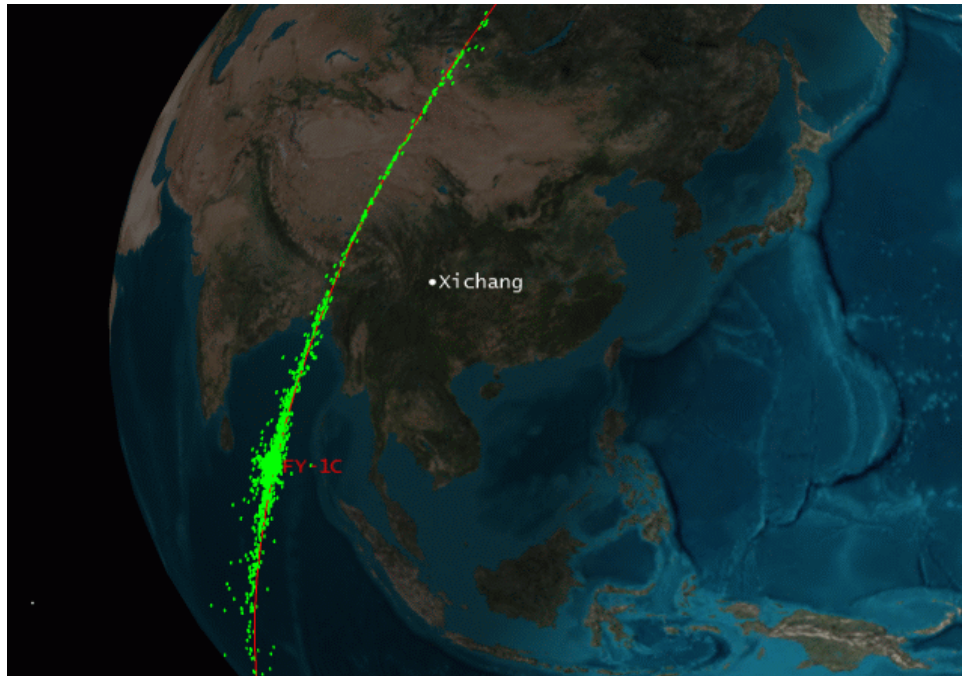
Figure 5.    FY-1C debris field five minutes after SC-19 impact (From [6])
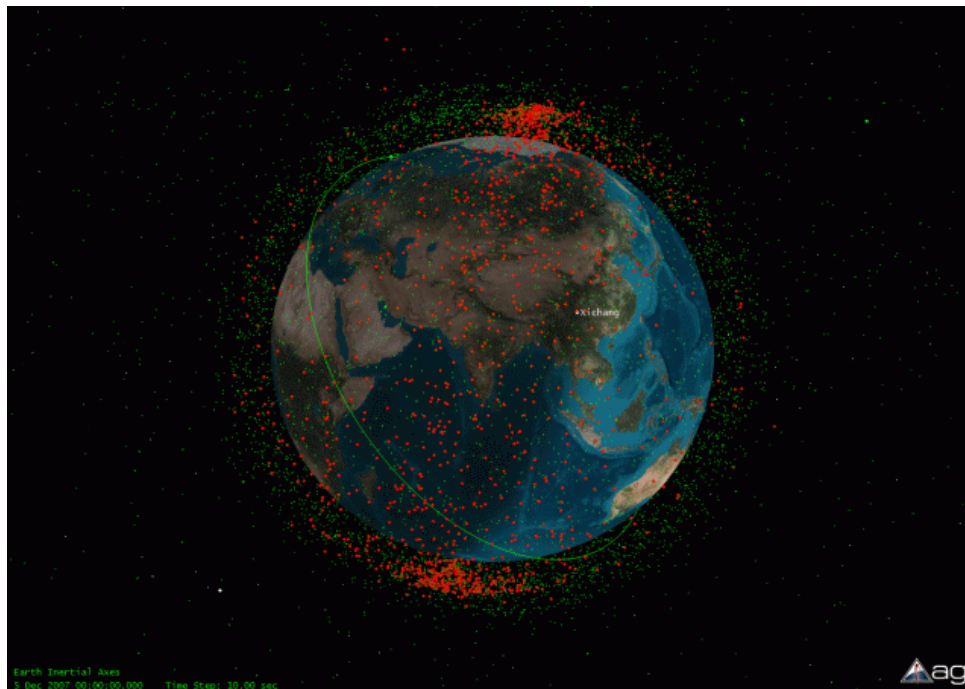


Figure 6.    Current debris field after FY-1C interception (From [6])

The second intentional spacecraft collision occurred on February 21, 2008 when a United States Standard Missile III (SM3) intercepted a failing U.S. satellite. Because the satellite's orbit had already decayed to a low altitude of 240km, the debris field caused from the collision reentered the Earth's atmosphere within a month [7].

The first unintentional collision of two spacecraft occurred on February 11, 2009. In this collision a dead Russian satellite, Cosmos 2251, collided with the Iridium 33 satellite at an orbital altitude of 790km [16]. This unprecedented collision created over 500 pieces of orbital debris and destroyed an active satellite, and brought space situational awareness, as well as the need to better track Earth orbiting objects into mainstream media.

## D.     CURRENT SSA ARCHITECTURE

In order to achieve space situational awareness, it is imperative to detect objects orbiting the Earth. Once the objects are detected, tracked, and catalogued, the data is then used to predict the object's orbital path and the potential for collisions. This section discusses the current SSA architecture of the United States.

The Space Surveillance Network (SSN) uses optical and radar sensors to detect, track, identify, and catalog all man-made objects orbiting the earth [8]. As of 1998, the resident space object (RSO) catalog contained over 10,000 objects [9]. The SSN tracks objects in low earth orbit (LEO) as small as 10cm.

### a.     *Ground-based Architecture*

The SSN consists of radar and electro-optical (EO) sensors. The three types of radar sensors are tracking, detection, and phased array [8]. The tracking radar, shown in Figure 7, the oldest type of radar used by the SSN, helps predict the target object's trajectory. Because the tracking radar sends a single beam of radar and physically tracks an object orbiting the earth as it crosses its field of view, it is only capable of tracking one object at a time and cannot search for an object. The second type of radar used is the detection radar, which sends a large area of radar energy and receives a return when an object crosses through it. The third type of radar used by the SSN is the

phased array radar that uses thousands of steerable transmit and receive beams and can track hundreds of targets simultaneously.  Phased array radars, shown in Figure 8 provide tremendous capability, but have extremely high cost and are complex to build, maintain, and operate.  While radar sensors send out energy and receive returns when an object intersects the beam, EO sensors passively gather light reflected off an object, forming an image.  EO sensors can only collect images when the imager is in the dark with clear skies and when sunlight is illuminating the target object.  An example of an EO sensor for SSA is shown in Figure 9.

Figure 7.    SSN Tracking radar, (From [8])

Figure 8.     Phased array radar (From [8])



Figure 9.     Electro-Optical sensor for SSA (From [10])

The three main categories of SSN sensors are dedicated, collateral, and contributing [8]. Dedicated sensors are those that have the primary mission of space surveillance and are owned by Air Force Space Command. Collateral sensors have a primary mission other than space surveillance, but are still an important part of the SSN. These sensors are also owned by Air Force Space Command, most of which were initially designed for missile warning. Finally, contributing sensors provide data to the SSN, and are owned by private contractors or other branches of the U.S. government. Figure 10 shows the locations of dedicated, collateral, and contributing sensors of the space surveillance network.



Figure 10.    SSN dedicated, collateral, and contributing sensor locations (From [8])

### b.    *Space-based Architecture*

The first space-based platform to perform space surveillance was the Space-Based Visible (SBV) program [9]. SBV was an EO camera payload on the Midcourse Space Experiment (MSX) satellite that launched in 1996 into a 900 kilometer altitude orbit, as seen in Figure 11. After first completing one year of technology demonstration, SBV began contributing to the SSN. The mission of SBV was to gather metric and photometric information on resident space objects (RSO). After years of service, SBV is no longer functioning.
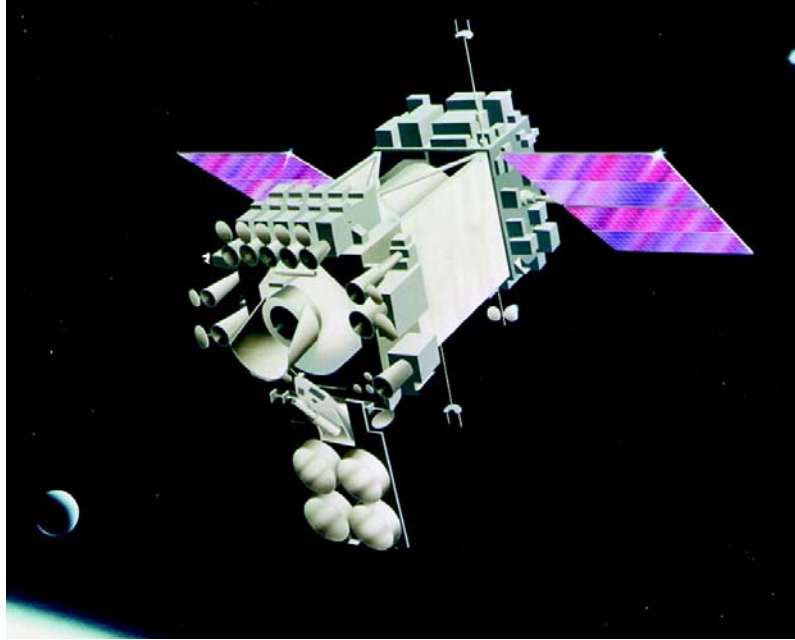
Figure 11.    Space-Based Visible (SBV) sensor on the Midcourse Space experiment (MSX) satellite (From [9])

Space Based Space Surveillance (SBSS) is now conducted with just one satellite, SBSS Block 10.  Shown in Figures 12 and 13 are the SBSS Block 10 payload and a simulated image of the spacecraft, respectively.  SBSS Block 10, launched in 2010, improved greatly on the performance of SBV [11].  Areas of improvement are sensitivity, capacity, detection probability, and the time to detect threats.

Figure 12.    SBSS Block 10 payload (From [11])



Figure 13.    SBSS Block 10 (From [11])

THIS PAGE INTENTIONALLY LEFT BLANK

## II.    FEASIBILITY OF USING 3U CUBESAT TO ENHANCE SPACE SITUATIONAL AWARENESS

The feasibility of using a 3U to enhance Space Situational Awareness is addressed here.  The Satellite Toolkit (STK) was used to run simulations of the SSA CubeSat with optical imager as it orbits the Earth, taking images of other satellites when there was a conjunction opportunity.

### A.    SIMULATION CONSTRAINTS

#### 1.    Orbital Parameters

The SSA CubeSat will be placed into an orbit by a launch vehicle.  For a representative orbit, the STK simulation used an altitude of 700km above the surface of the Earth at an inclination of 63 degrees.

#### 2.    Imaging Satellite Constraints

In order for the optical imager to take an image, the SSA CubeSat must be completely in the Earth's shadow, called umbra, while the target satellite must be in full sunlight, as seen in Figure 14.
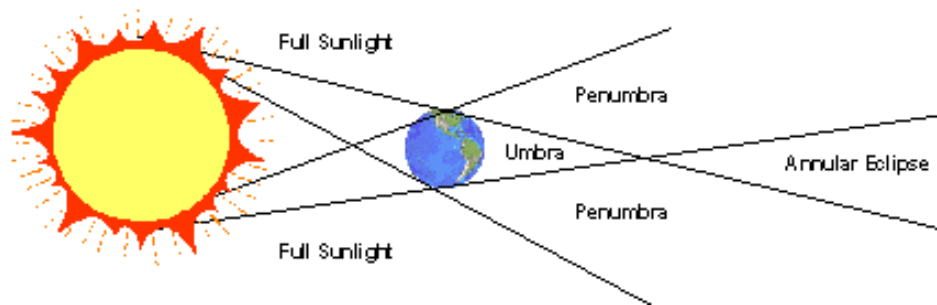


Figure 14.    Depiction of umbra and full sunlight (From [12])

The STK simulation included several other constraints on the spacecraft.  The imager's field of view was taken into account; however, it was not used as a constraint because of the spacecraft's attitude control system.  For instance, because the satellite has the ability to maintain a particular attitude while imaging an object, it was assumed that

the SSA imager is pointed at the target satellite, maintaining the requisite sensor pointing accuracy. The light-sensitive optics used in the imager can be damaged by looking at bright objects such as the sun or the sun's reflection on the Earth. Therefore, the imager has a solar exclusion angle of 30 degrees and an Earth exclusion angle of 85 degrees to ensure that neither bright object comes into the field of view of the imager. The solar exclusion angle, as seen in Figures 15 and 16, is the angle between the sun and a target satellite, as viewed from the imaging satellite. For example, if a target satellite was within the solar exclusion angle, because the satellite attitude control system would be programmed to not point the imaging sensor inside the exclusion angle, it would not take an image that particular satellite.
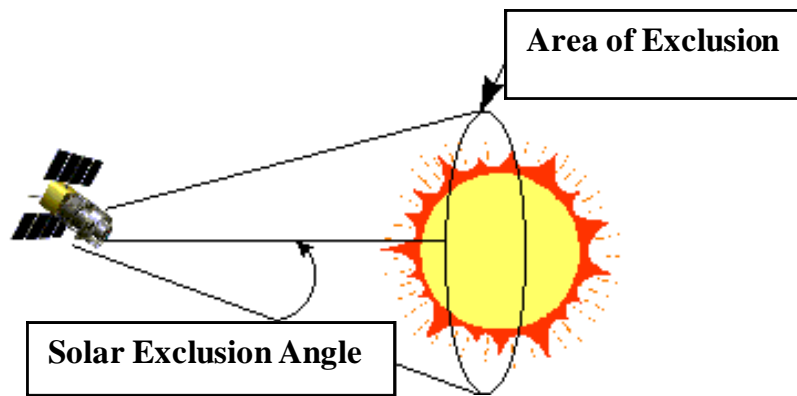


Figure 15.    Solar exclusion angle (from [12])
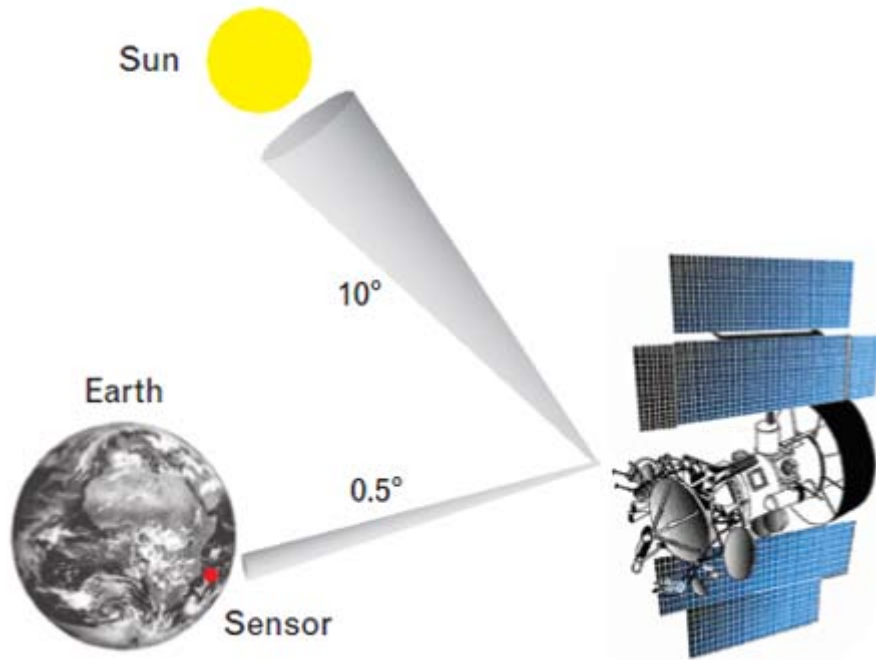
Figure 16.    Example of sun angle and imager field of view (From [13])

Additional physical constraints applied to the STK simulation were the maximum range and crossing velocity between the SSA CubeSat and the target satellite.   The crossing velocity is the relative velocity between the imaging and target satellite.  For the purposes of this analysis, the maximum range for the useful goal was chosen to be 300km.   Similarly, the maximum crossing velocity between satellites is chosen to be three kilometers per second, though useful data is gained from a conjunction with crossing velocity between satellites of less than 10km per second.   Because both the imaging and target satellite are in LEO, the maximum expected crossing velocity is over 14km per second, while the average relative velocity is between nine and ten km per second [14].

**B.    SIMULATION RESULTS**

Several STK simulations were run, each with varying constraints and parameters. To get a representative sample of one year in orbit, the simulations were each run from 01 January 2011 through 31 December 2011.  Propagating satellites for an entire year is

15

computationally demanding and resource intensive.  The objects used in STK were unclassified active satellites only.  This limited the possible conjunction opportunities by precluding classified national systems, as well as orbital debris maintained in the SSN catalog, although it provided a good representative sample of imaging opportunities.

In the first STK simulation the maximum range of the imaging satellite was set to 1,000km.  This not only took more than four hours to run, but it also yielded many conjunction opportunities, proving that at least one conjunction per day was possible. The maximum range was then decreased from 1,000 to 100km, yielding fewer conjunction opportunities.  The third simulation included a maximum range of 300km, which is a compromising balance between minimum range with few conjunctions and maximum range with many conjunction opportunities.

The STK satellite database was first filtered to display only satellites with an apogee less than 2,000km in order to have a possible conjunction opportunity.  To reduce computation time, all of the filtered satellites were not added to the simulation at the same time.  Eight iterations of this simulation were run for one year, each with a portion of the filtered satellites.  A list was made of any satellite that had a conjunction opportunity at least once during the year.  After eight iterations, the compiled list of 159 conjunction-capable satellites was used in another simulation.  Table 1 shows a representative sample of satellites that produced a conjunction opportunity in February, 2011 at a range less than 300km.

| SSA imaging opportunity | Time (UTCG) | Range (km) |
| --- | --- | --- |
| SAUDICOMSAT_5_31124 | 1 Feb 2011 02:20:47.902 | 280.30 |
| UGATUSAT_35869 | 1 Feb 2011 18:49:39.314 | 293.18 |
| METEOR-M_1_35865 | 2 Feb 2011 09:37:56.131 | 154.42 |
| VO-52_28650 | 2 Feb 2011 17:51:36.710 | 283.07 |
| COROT_29678 | 2 Feb 2011 23:21:01.487 | 264.02 |
| COSMIC-3_FM2_29052 | 3 Feb 2011 07:01:55.423 | 159.66 |
| TATIANA_2_35868 | 3 Feb 2011 11:58:41.520 | 109.65 |
| STERKH_2_35866 | 3 Feb 2011 16:54:39.435 | 230.96 |
| SLOT_B8_25416 | 5 Feb 2011 12:15:22.012 | 297.09 |
| ORBCOMM_FM19_25415 | 5 Feb 2011 22:08:12.953 | 288.93 |
| TATIANA_2_35868 | 6 Feb 2011 05:49:55.932 | 110.10 |
| THEOS_33396 | 12 Feb 2011 18:15:23.278 | 224.07 |
| THEOS_33396 | 15 Feb 2011 08:49:08.670 | 160.00 |
| THEOS_33396 | 17 Feb 2011 23:22:56.082 | 130.64 |
| SPOT_4_25260 | 18 Feb 2011 09:15:26.590 | 297.22 |
| FORMOSAT-2_28254 | 19 Feb 2011 03:21:58.059 | 212.41 |
| THEOS_33396 | 20 Feb 2011 13:56:39.470 | 123.10 |
| SPOT_4_25260 | 20 Feb 2011 23:49:19.379 | 267.70 |
| THEOS_33396 | 23 Feb 2011 04:30:25.082 | 146.87 |
| SPOT_4_25260 | 23 Feb 2011 14:23:08.471 | 238.77 |
| ORBCOMM_FM05_25117 | 25 Feb 2011 11:24:50.997 | 64.31 |
| SLOT_A1_25117 | 25 Feb 2011 11:24:50.997 | 276.45 |
| ORBCOMM_FM16_25417 | 25 Feb 2011 17:59:43.564 | 223.34 |
| THEOS_33396 | 25 Feb 2011 19:04:19.795 | 142.90 |
| SPOT_4_25260 | 26 Feb 2011 04:57:03.153 | 261.98 |
| THEOS_33396 | 28 Feb 2011 09:38:14.336 | 179.00 |

Table 1.    Representative list of satellites with conjunction opportunity at a range less than 300km during February 2011

All 159 satellites were entered in a single simulation, which was run in one month increments to determine the conjunction opportunities possible in a month, as shown in Figure 17, where the cyan orbit track is the SSA CubeSat, labeled as SSA, and the dark blue lines represent the orbit track of the other 159 satellites.
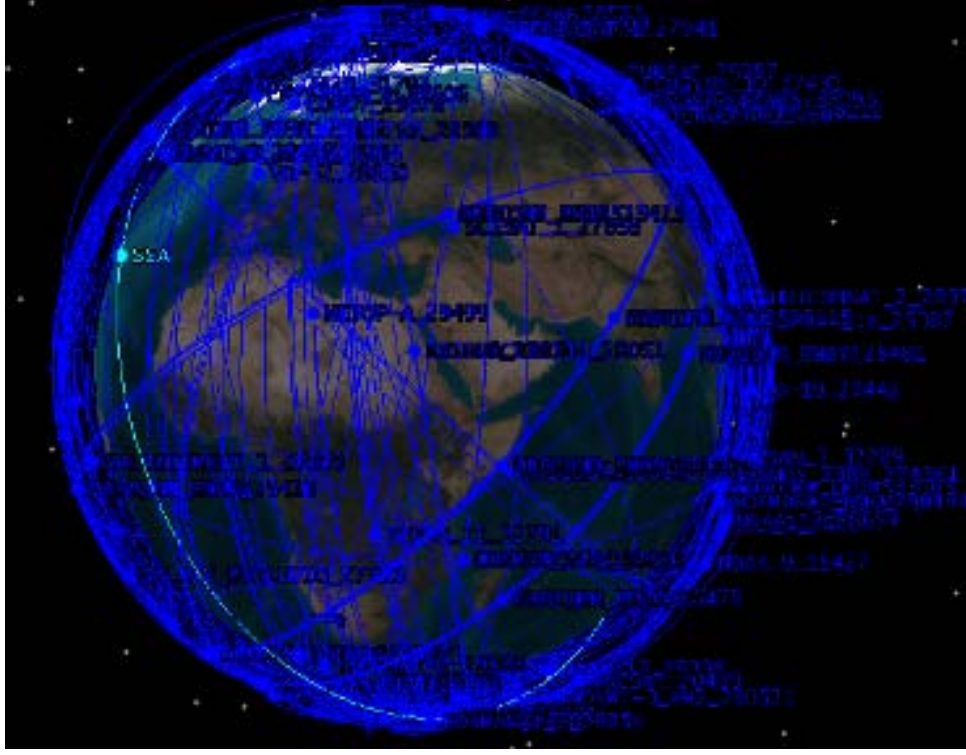
Figure 17.    STK simulation, 3D image

The constraint for the maximum relative velocity between the imager and the target satellite is 10 kilometers per second, but less than three kilometers per second is preferable.  Since satellites in LEO are travelling at roughly seven and a half kilometers per second, the maximum relative velocity is 15 kilometers per second, assuming the two satellites are in similar orbits with opposing directions.  For example, if the target satellite and the SSA imager are each travelling seven and a half kilometers per second and have a crossing angle of 90 degrees, the relative velocity would be $7.5\frac{km}{s}\sqrt{2}=10.6\frac{km}{s}$. Therefore, the crossing angle between the imager orbital velocity and the target satellite orbital velocity should be less than 90 degrees.

Figure 18 shows the two dimensional depiction of both satellites during a conjunction, where $\vec{R}_1$ and $\vec{V}_1$ are the position and velocity vectors for the SSA satellite, $\vec{R}_2$ and $\vec{V}_2$ are the target satellite's position and velocity vectors relative to the center of

18

the Earth, and $\vec{R}_{12}$ is the relative position between the satellites. The relative velocity between the two satellites is given by $\vec{V}_{\text{Relative}} = \vec{V}_2 - \vec{V}_1$, as shown in Figure 19.
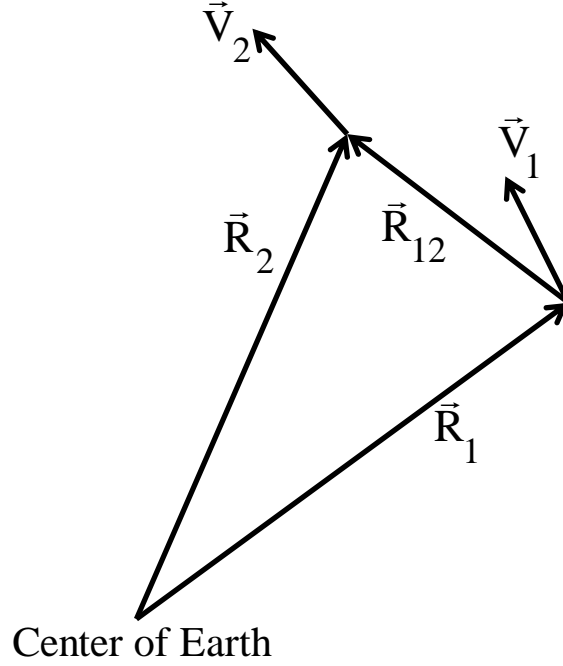


Figure 1.    Satellite position and velocity vectors used for calculation

The relative velocity, $\vec{V}_{\text{Relative}}$, between the two satellites has both parallel and perpendicular components to the line of sight between the two satellites. The line of sight vector, $\vec{R}_{12}$, is shown in Figure 18, and is $\vec{R}_{12} = \vec{R}_2 - \vec{R}_1$. The parallel component of relative velocity is calculated by taking the dot product of the relative velocity and $\vec{R}_{12}$ [19], as shown in Equation 1. The perpendicular component of velocity is what creates the relative difference in position of the target satellite that is imaged as a streak by the CCD, and is the desired and constraint-driven velocity component. The perpendicular component of relative velocity, $\vec{V}_{\text{Perpendicular}}$, is found using Equation 2 as follows:

$$\vec{V}_{\text{Parallel}} = \frac{\vec{V}_{\text{Relative}} \bullet \vec{R}_{12}}{\left| \vec{R}_{12} \right|} | \qquad\qquad\qquad \text{(Equation 1)}$$

19

$$\vec{V}_{Perpendicular} = \sqrt{\vec{V}_{Relative}{}^2 - \vec{V}_{Parallel}{}^2} \qquad \text{(Equation 2)}$$
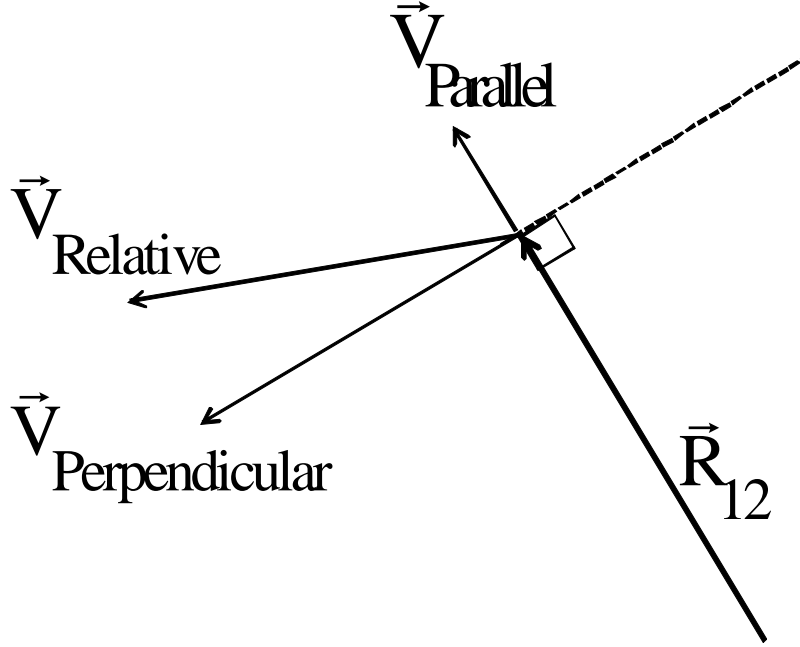


Figure 19.   Vector geometry used for calculating relative and perpendicular velocity

An example of a conjunction at a distance of less than 300km with a relative velocity less than three kilometers per second was with the satellite COSMOS_2428 on June 5, 2011.  Cosmos_2428, launched on June 29, 2007 into an orbit with an apogee of 880km and perigee of 850km and an inclination of 71 degrees, is a Russian electronic intelligence satellite [18].  Table 2 shows the position and velocity of the two satellites during the conjunction.  For this conjunction opportunity, the relative velocity between the imager and Cosmos_2428 was found to be 1.8 kilometers per second.  Therefore, this conjunction should provide a useful image.

| J2000 Position and Velocity | SSA | COSMOS_2428 |
|---|---|---|
| X (km) | 3929.89 | 4186.88 |
| Y (km) | -2672.61 | -2795.53 |
| Z (km) | -5245.29 | -5188.85 |
| Vx (km/sec) | 6.24 | 5.84 |
| Vy (km/sec) | 1.89 | 0.28 |
| Vz (km/sec) | 3.71 | 4.57 |

Table 2.    Position and velocity used for crossing velocity used for sample calculation

Once the tangential component of relative velocity is determined to be less than three kilometers per second, the next step is to ensure the streak imaged by the CCD will fit in the imager's three degree field of view during the one second exposure. This calculation solves for the angle subtended by the satellite streak, where one side of the triangle is the range between the two satellites at the time of the conjunction (296km), and the other side is the 1.8km Cosmos_2428 travels in the tangential direction, relative to the imager, in one second. The angle is calculated to be 0.35 degrees, using Equation 3, which is smaller than the imager's three degrees field of view. As a result, the streak will easily fit inside the imager's field of view.

$$\theta = \sin^{-1}\left(\frac{1.8km}{296.4km}\right) \qquad \text{(Equation 3)}$$

THIS PAGE INTENTIONALLY LEFT BLANK

# III. INTEGRATING SPACECRAFT BUS AND PAYLOAD

For NPS to properly integrate a payload with the C2B, it is important to understand both the payload and the spacecraft bus. This thesis takes an initial, overview look at both the bus and payload to prepare for their eventual integration. The space available inside the spacecraft for the payload, the payload bay, is roughly half of the spacecraft, or 1.5 U, which is 9.75cm x 9.75cm x 15.0cm, as seen in Figure 20. The payload bay must contain the payload and all required interfaces.



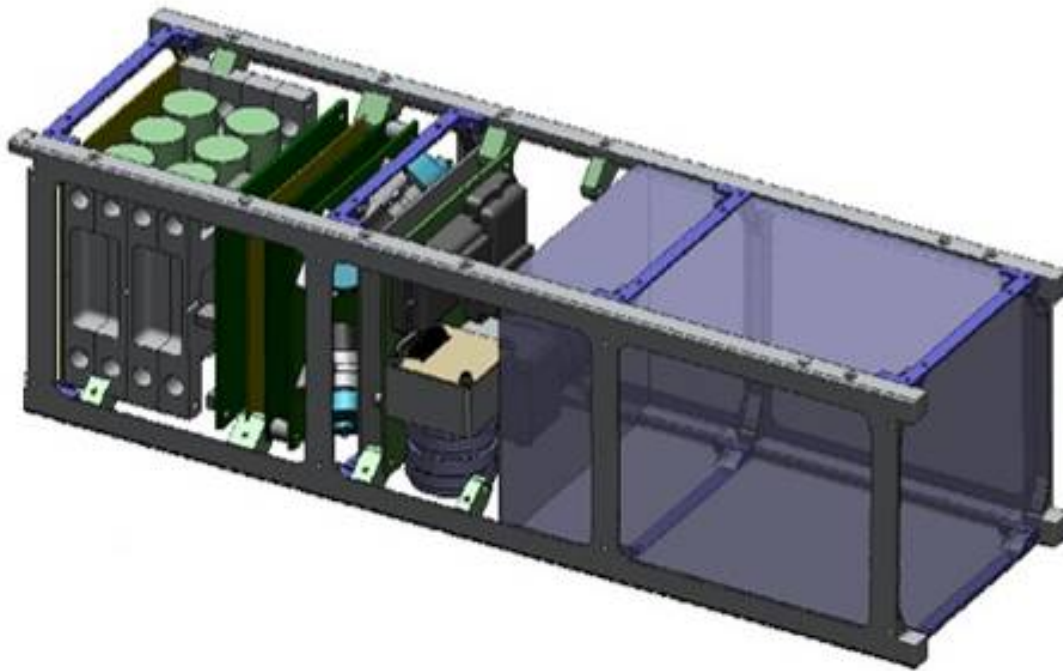Figure 20.    Spacecraft layout and payload dimensions (From [15])

The two main components of a spacecraft are the bus and payload. The payload is the main experiment or instrument that performs the spacecraft's mission. The spacecraft bus contains the rest of the spacecraft, specifically the structure, attitude determination and control subsystem, power generation and storage, and communications.

**A.     COMPONENT INTEGRATION**

**1.     Conceptual Spacecraft Block Diagram**

The C2B provides power and data to any payload.  The LLNL payload includes a payload processor board, called the imager board and formerly known as the BC500, and a GPS unit (OEMV-1G).  The C2B communicates directly with the payload processor board and GPS receiver.  The payload processor board and camera communicate with the C2B via serial data.  The payload processor processes information from the camera and GPS receiver, then sends information to the C2B for storage or transmitting to the ground.  Figure 21 shows the conceptual spacecraft block diagram, created using Microsoft Visio.  The C2B is shown on the left..  The payload processor receives the raw data from the optical imager and GPS receiver, then processes the information and transfers the data to the C2B.  The solid lines represent power distribution, while the dashed lines represent data links.
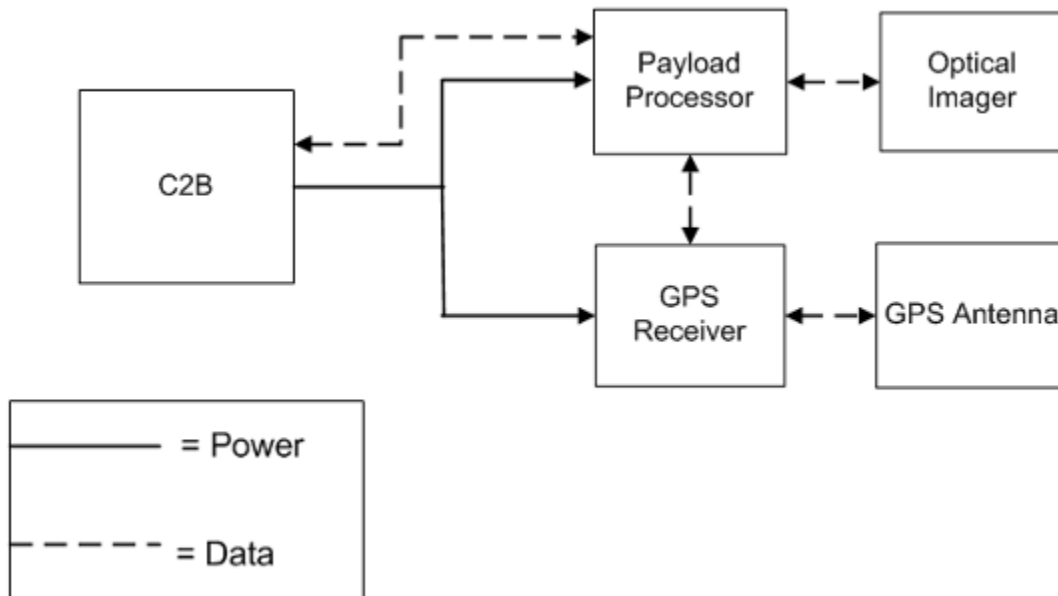
Figure 21.    Functional spacecraft block diagram of spacecraft bus and payload

## 2. Spacecraft Component Connections

After understanding the functional block diagram of the spacecraft bus and payload, it was important to know how each component connects with each other. As shown in Figure 22, the C2B provides one data cable and one power cable. The payload, on the far right, has three connectors, where two are for the payload processor board and one is for the GPS receiver. The dashed box in the center of the Figure represents the required interface between the C2B and the payload. By noting the different size of the connectors, with a 20-pin data connector from the spacecraft, and both 20-pin and 30-pin data connectors on the payload, it is easy to see the requirement for a good interface to enable the spacecraft bus and payload to operate and communicate with each other. The lines drawn between the connectors are representative and may not be actual data paths.
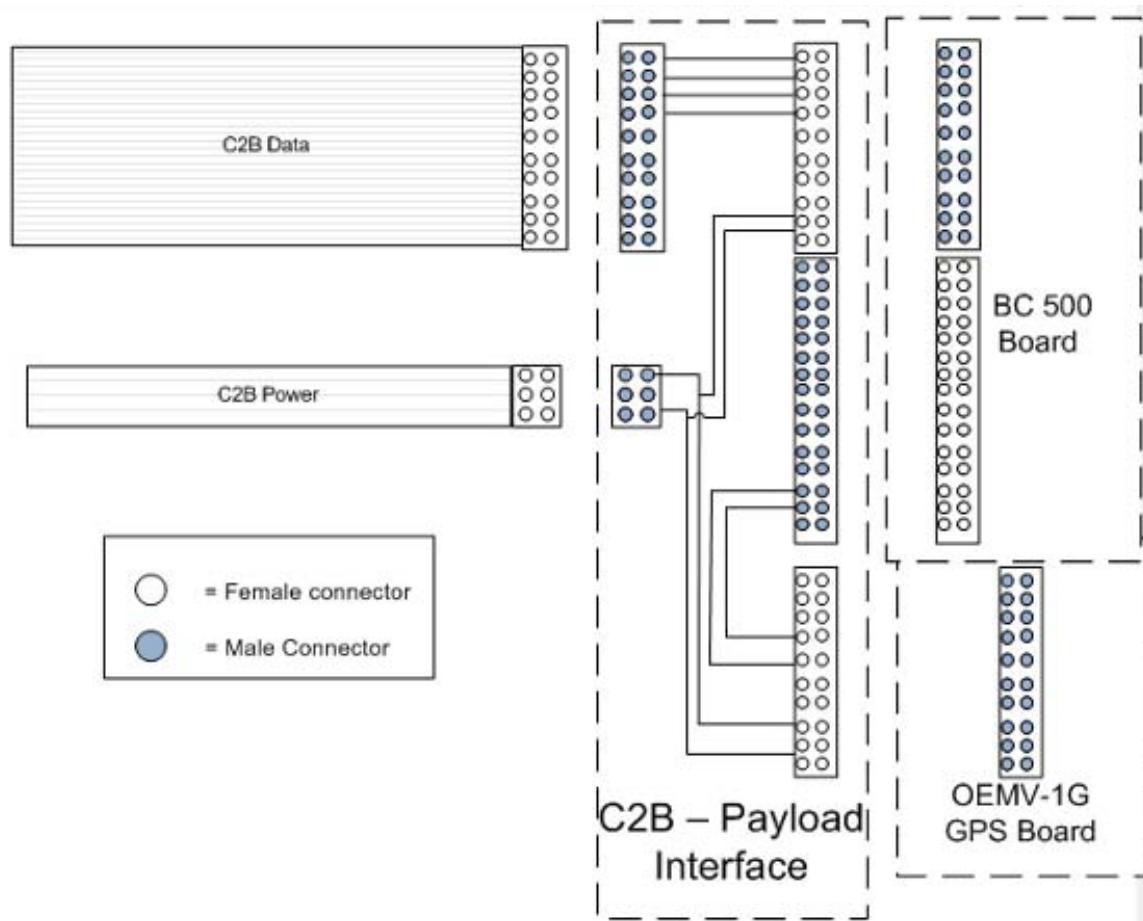


Figure 22.    Spacecraft bus and payload connectors

25

Two methods of creating the connections between the bus and payload were evaluated.  The first method requires cutting and splicing the wires to create the required connections.  Since there are five cables required to complete the integration process, using the cut and spliced wiring procedure was labeled the penta-harness.  The second integration method uses a printed circuit board (PCB) to connect the bus and payload.

Creating the penta-harness requires snipping the wires, stripping the sheath from the wire, and then soldering the wire to another wire to properly route the signals. Figures 23 through 25 show the author stripping the snipped wire, labeling the wires, and displaying the relative size of the wire.



Figure 23.    Stripping the sheath off wires of the 20-pin C2B data cable

Figure 24.    Labeling the wires of the 20-pin C2B data cable



Figure 25.    Demonstrating the small size of the wire (only 0.255 mm diameter) of the
20-pin C2B data cable [17]

The second method of integrating the bus and payload uses a PCB. The PCB holes are built into the board, allowing the connectors and cables to be soldered directly into the board. This creates more sturdy contacts, eliminates the need to splice wires together, and easily allows varying connector cables length. The size of the PCB is not much larger than the size of the connectors themselves. The PCB's mass is estimated to be 30 grams, similar to the mass required to create the penta-harness.

After developing both the penta-harness and PCB for integration, this project is planning to move forward with the PCB instead of the penta-harness. Several factors were considered when choosing between the two integration methods. First, the small size of the 30 gauge wire, only 0.255 mm diameter [17], makes cutting, stripping, and splicing difficult. Second, when splicing one wire from a connector to another wire from another connector, the splice must be soldered to ensure good connectivity. When the solder solidifies it becomes stiff, no longer allowing the wire to be flexible, and creates a potential weak point where the wire can snap if bent. The third reason the PCB was chosen over the penta-harness is because three connects on two boards require power from the C2B. With the penta-harness, all three connectors would have to be powered, adding to the complexity of the integration. With the PCB, however, power is distributed easily to both boards. The final and most critical reason why the PCB was chosen over the penta-harness is the requirement for an active component, the level shifter, discussed later, which requires a power source to enable communication between the C2B and payload.

The first step to create the integration board (I-board) was to determine the components that needed to connect to the board. As mentioned previously, there are two inputs coming from the C2B, the 20-pin data cable and the six-wire power cable. Therefore, the first two components on the I-board were the connectors required to attach to the C2B data and power source. These two connectors will be soldered into the I-board so the associated cables can plug in to the board. The next three components that

need to be attached to the I-board are the two cables, one twenty-pin and one thirty-pin for the payload, as well as the GPS 20-pin cable. These three cables will be soldered into the I-board.

Before laying out the wiring on the PCB using Altium Designer, a pseudo PCB I-board was created in order to become familiar, and alter if necessary, the layout of the PCB. The pseudo PCB was created using the 3-D modeling programNX6. Rectangular slots were used for connector insertion into the board. Figure 26 shows a screenshot of the pseudo PCB using NX6, where the dimensions are 2cm by 3cm.
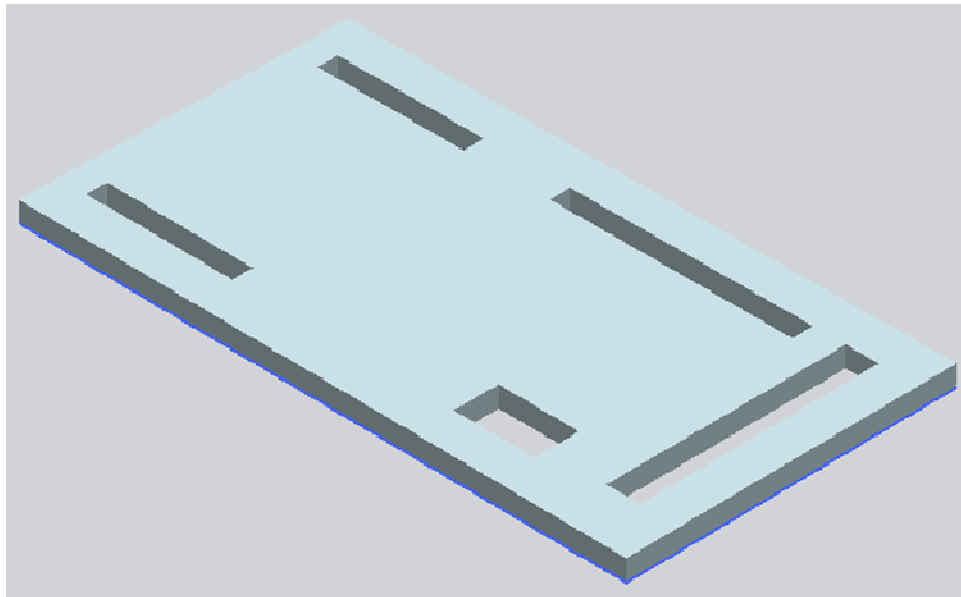


Figure 26.    Screenshot of pseudo PCB created in NX6

Figure 27 shows the PCB I-Board with attached C2B data and power connectors, both payload cables, and the GPS cable. The end of the payload and GPS cables that is not attached to the I-board will connect to the payload (in the direction of the arrow shown in the Figure).

Figure 27.    Pseudo PCB I-board with C2B data and power (left), payload cables (right), and GPS cable (bottom)

Figure 28 shows the underside of the pseudo PCB I-board.  The C2B data and power cables are on the right, the payload cables are on the left, and the GPS cable is at the bottom.  On the PCB, the pins protruding through the board will be soldered in place.
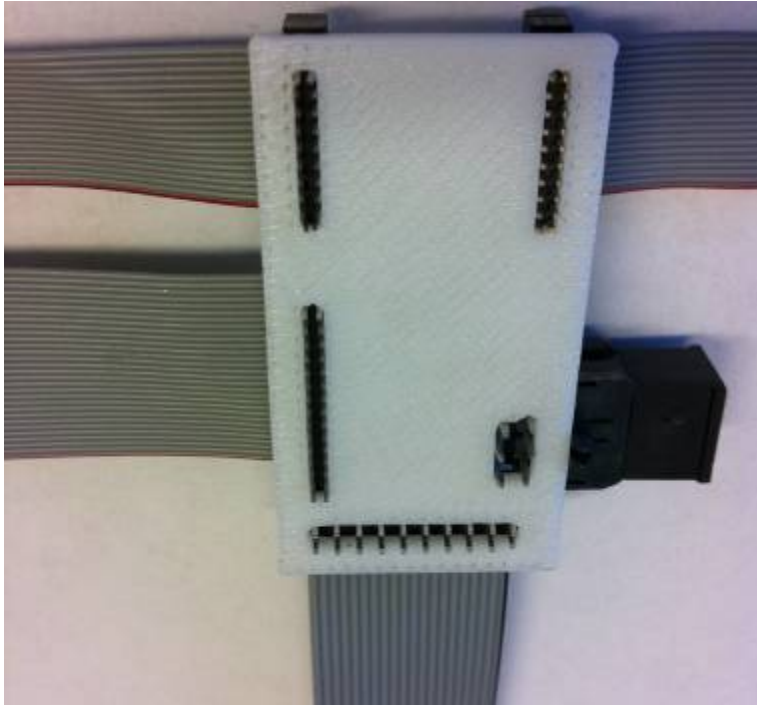
Figure 28.    Underside of pseudo PCB I-board, where the C2B data and power (right), payload cables (left), and GPS cable (bottom)

It is extremely important for the connectors on the I-board to be as secure as possible.  While the two cables for the payload and the cable for the GPS board will be soldered directly into the I-board because they are the terminal end (male), the C2B data cable the socket end (female) cannot be soldered directly to the PCB.  Therefore, a locking mechanism may be used on the board, as seen in Figure 29.  The two connectors on the payload and the connector on the GPS board also need to be securely attached, however, NPS is not responsible for the payload board or the GPS board.   The requirement and implementation for the securing mechanism of the payload and GPS boards needs to be determined.
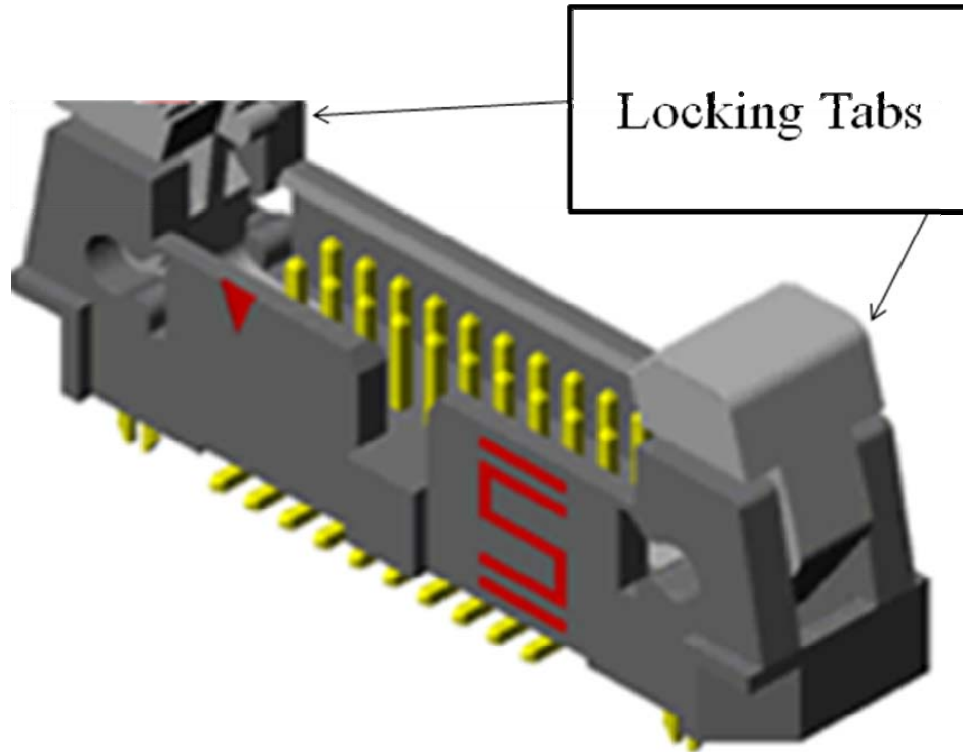
Figure 29.    Locking Mechanism used on I-board to connect and secure C2B data cable to PCB (From [20])

### 3.    Spacecraft Bus Emulator

The C2B emulator is intended to facilitate initial testing the payload without requiring the use of an actual spacecraft bus, engineering design unit (EDU) or flight unit, which is expensive and limited in availability.  In addition to the connectors and cables mentioned in the previous section, laboratory equipment was required to create the emulator.  The power supply chosen was the Agilent E3632A, which can provide two different power levels as required by the payload.   The RS422, providing serial communication between the payload and bus, was purchased from B&B Electronics.  The digital channels from the bus provide the inputs and outputs for the payload.   These digital channels are provided by Measurement Computing Company's Data Acquisition (DAQ) module.

Using Microsoft Visio, a block diagram of the C2B emulator was created, as seen in Figure 30.  The dashed box on the left shows the laboratory equipment used to provide

the power and data. The two boxes on the right of the figure show the three payload connections. The connections in the center of the diagram provide the necessary integration of the bus and payload, according to the current documentation provided by LLNL. Although the documentation is not yet complete, the integration concept is straightforward. The need is to understand the bus and payload well enough to ensure signal compatibility and operability.
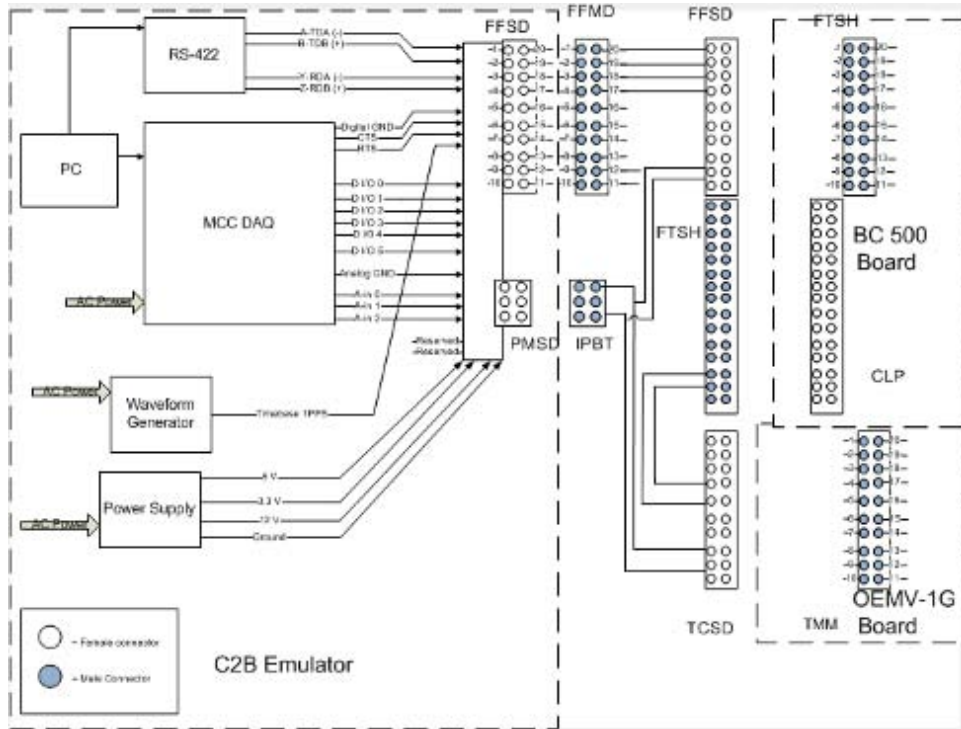


Figure 30.    C2B emulator and payload integration block diagram

### 4.    Payload Extender

The payload extender is used to connect the spacecraft bus and payload without requiring the payload to be placed inside the spacecraft. This allows easier access to the payload for troubleshooting and reduces wear and tear on the components. The payload extender consists of cables with the same connector ends used for the payload and bus integration. For instance, instead of a four inch cable used inside the spacecraft, a 12 inch transfer cable is used to lengthen the connection to connect to the payload outside the bus. Figure 31 shows the 12 inch transfer cables used to create the payload extender.

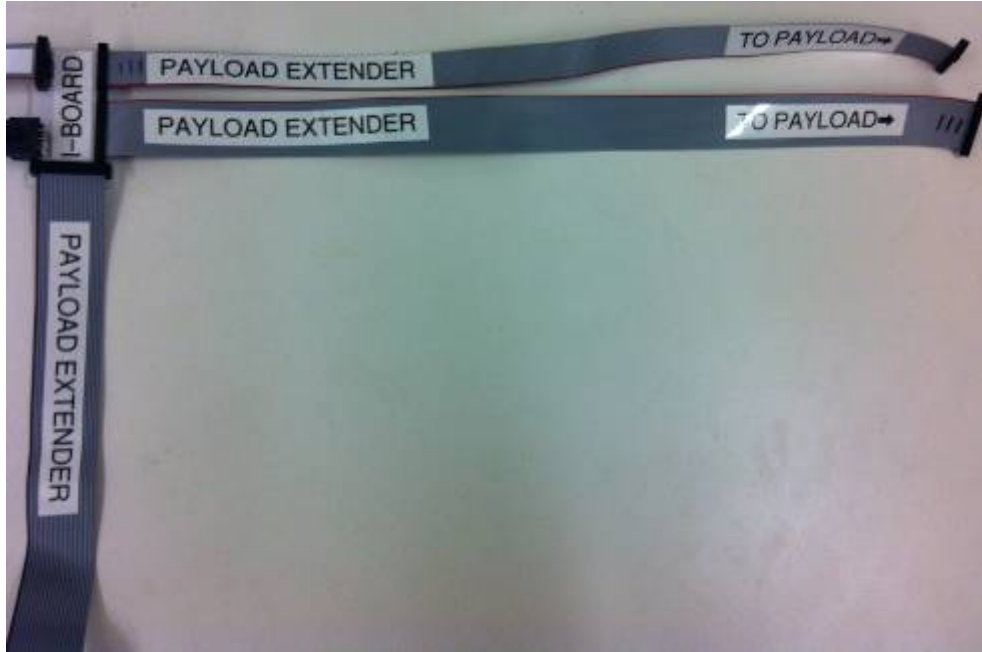Figure 31.    Payload extender using 12 inch transfer cables

## B.    TESTING COMPONENTS

The first test of the spacecraft interface simulator was the serial communications between the spacecraft bus and payload.  This test used the RS422 portion of the C2B emulator and the communication terminal program TeraTerm.  The C2B emulator was connected to a computer's communications port using the RS422, and the emulated payload with RS232 was connected to a different communications port on the same computer.  Using Tera Term, a message was sent from the emulated bus to the emulated payload.  Initially, the communication did not work between the C2B RS422 and the payload RS232.  The communication between RS422 and RS232 did not work because the two methods of communication are incompatible due to their design.  The RS422, using two wires to transmit and two wires to receive, uses differential voltage.  This means that the RS422 needs both a positive voltage and a negative voltage to form a binary digit.  The RS232, on the other hand, uses single ended output and input, requiring only one wire for transmitting and one wire for receiving.  This single ended output is achieved using positive only voltage, using a low voltage for a binary zero and a higher voltage for a binary one.  Because the RS232 only registers positive voltages, it does not

interface properly with the negative voltages of the RS422. The solution is to use a level shifter to allow communications between the bus' RS422 and payload's RS232. Requiring the level shifter necessitates using an interface PCB vice the penta-harness. The level was designed and put together by NPS lab manager David Rigmaiden. Figure 32, also created by David Rigmaiden, demonstrates how the MAX3070E level shifter enables communication between the four wire RS422 and the two wire RS232. Figure 33 shows the use of the level shifter on a prototype-board required to facilitate RS422 to RS232 communication. Figure 34 shows the RS422 portion of the C2B emulator connected with two separate communication ports of a computer
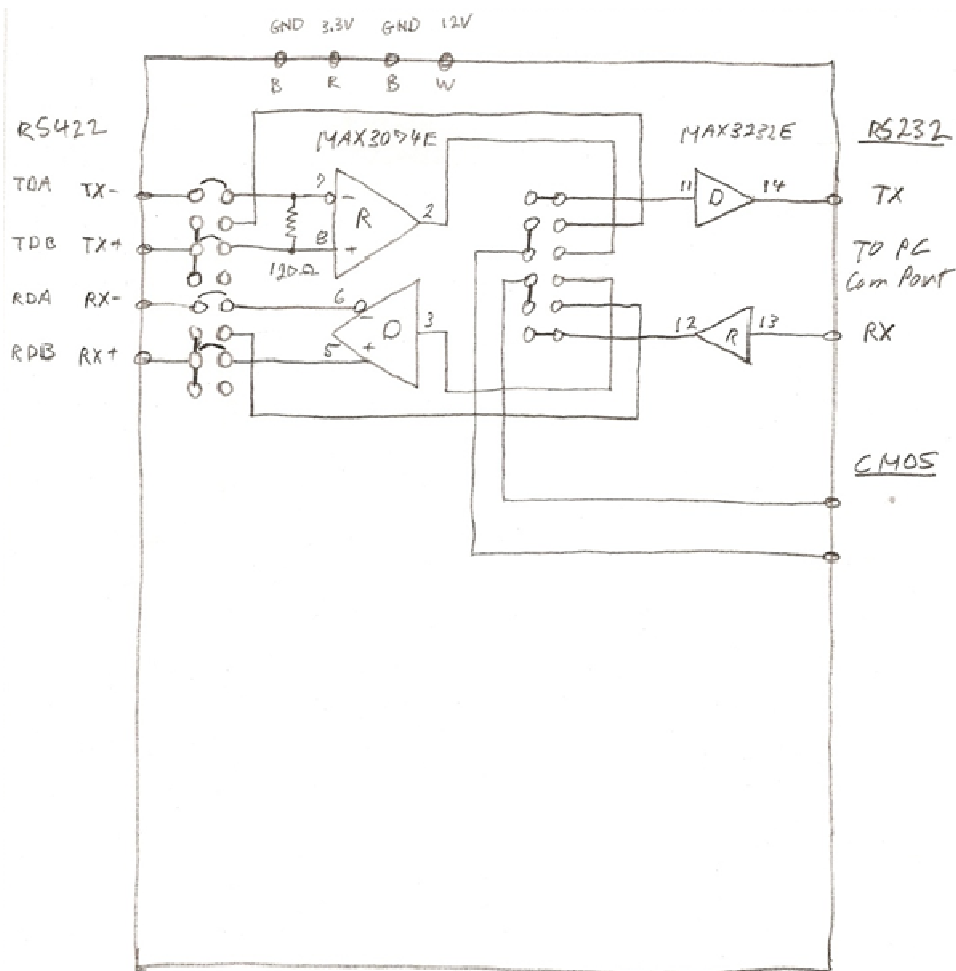


Figure 32.    Schematic of how the MAX3070E level shifter enables communication between RS422 and RS232

Figure 33.    C2B RS422 (left) to payload RS232 (right) using level shifter (center)
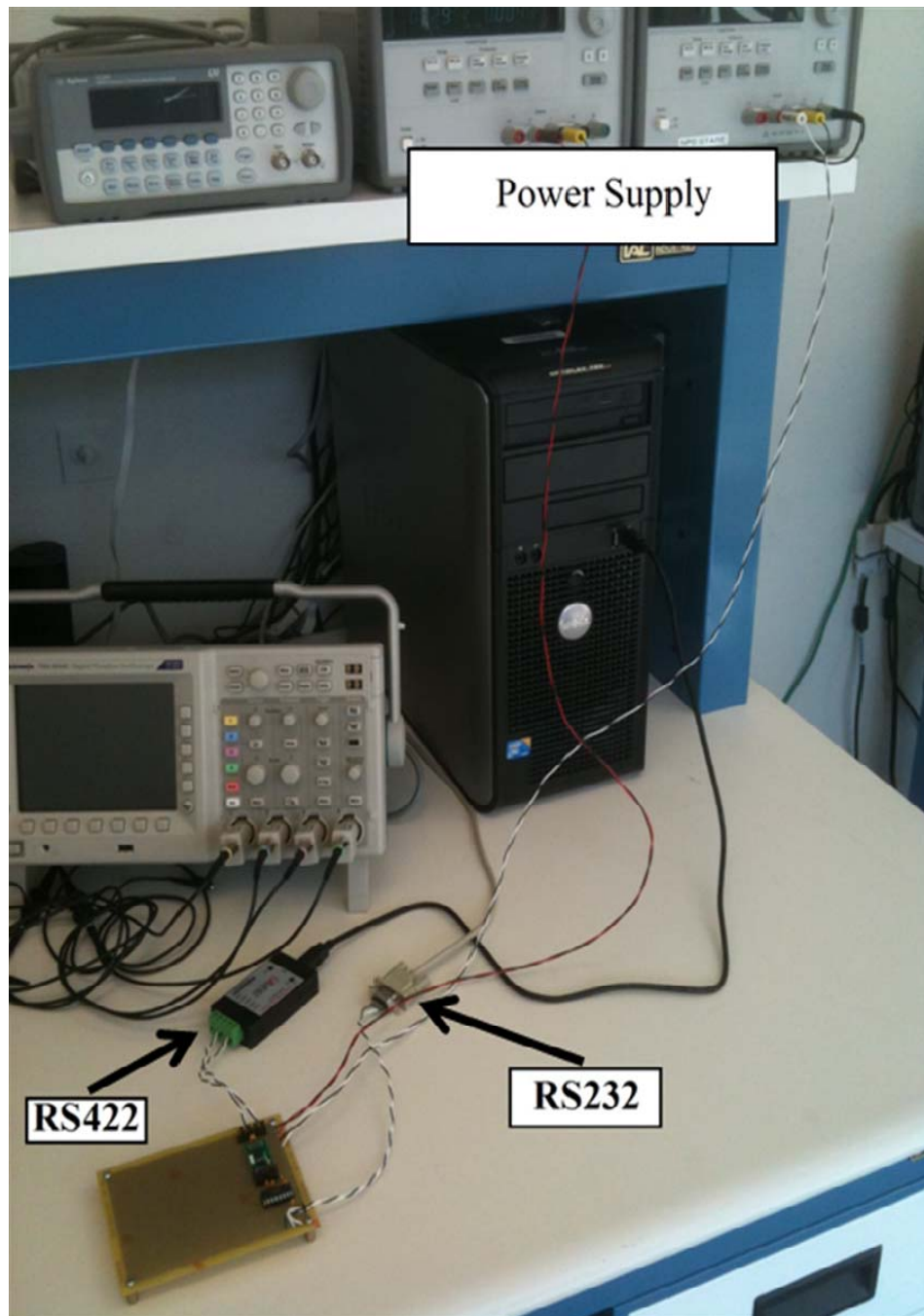
Figure 34.    C2B RS422 to payload RS232 communication test

After verifying the level shifter worked to enable communication between the C2B and the payload, a preliminary graphical user interface (GUI) was created by NPS SSAG Research Associate Jim Horning. This GUI uses the same communication ports as

before, but includes the Measurement Computing Corporation (MCC) DAQ, is programmed to emulate the data provided by the C2B. Figure 35 sh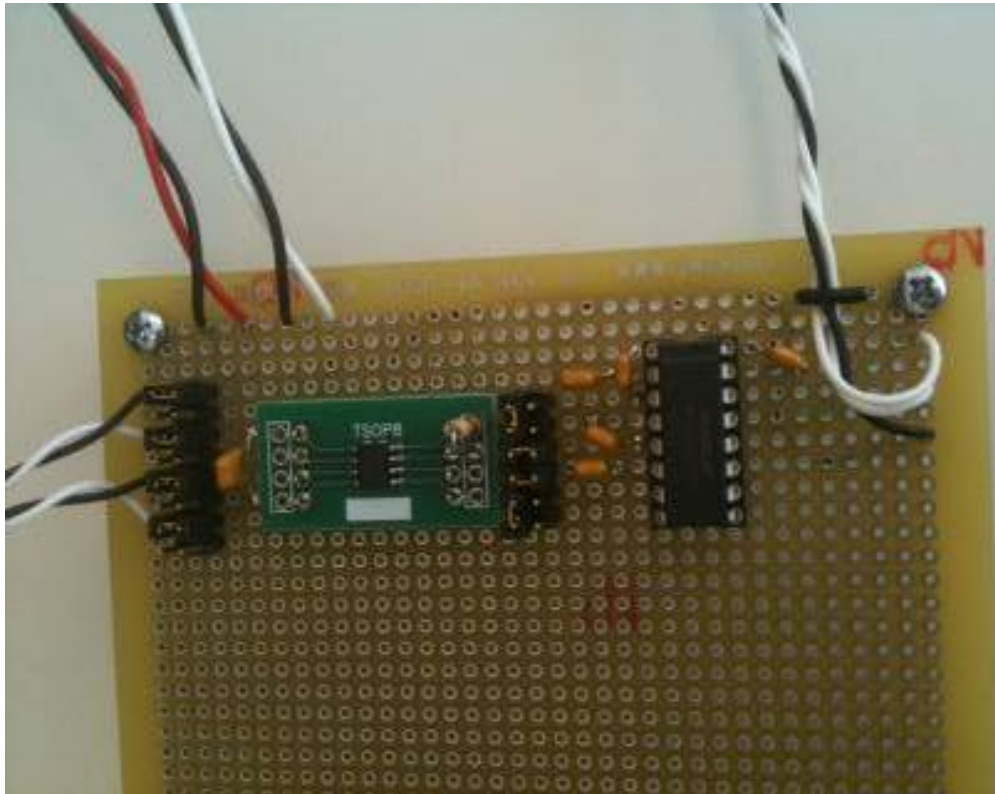ows the DAQ connected to the GUI via communication port. In the GUI window, the user can select the desired Digital Input/Output (DIO) on the DAQ. The illuminated red light next to a DIO means, that DIO is being used. In addition to enabling and disabling selected DIOs, the GUI allows the user select files to transfer between the C2B and payload. The received file is also saved in specified locations.
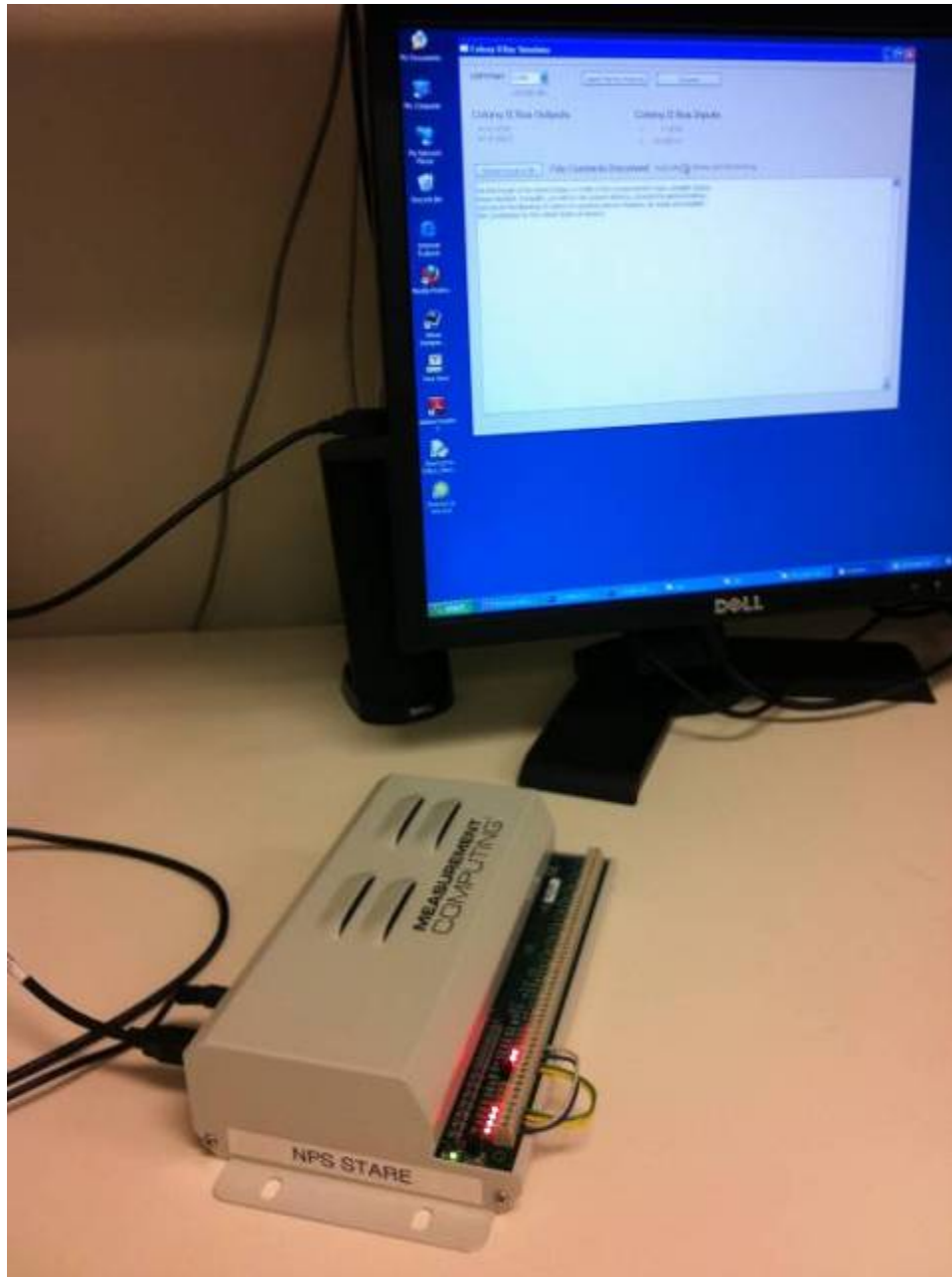
Figure 35.    MCC DAQ, controlled by GUI, connected to communication port

Figure 36 shows the GUI for both the C2B and the payload, with none of the DIO turned on.  To test communication between bus and payload, a sample code sent from the C2B to the payload, then from the payload to the C2B.  In this case, a sample text file

was sent, as seen below.  Because the text was successfully sent and received from both the emulated C2B and payload, it is seen in both GUI screens.
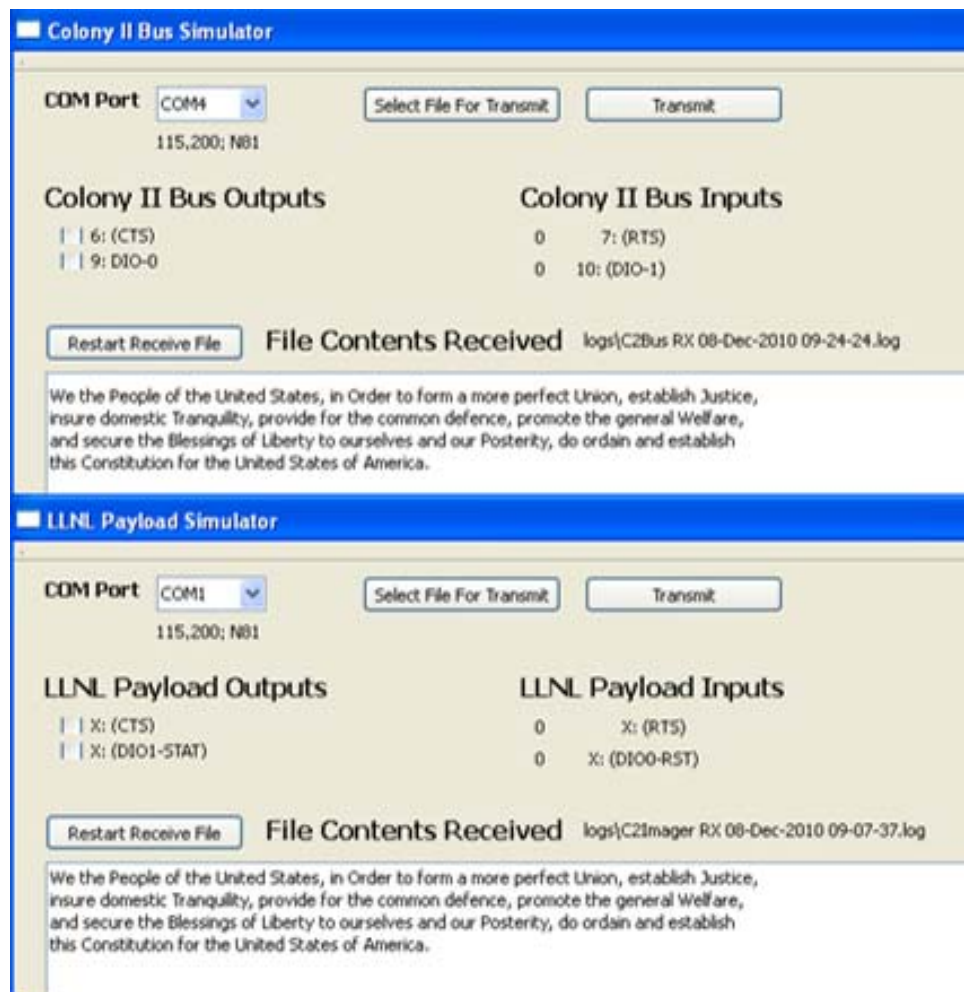


Figure 36.    C2B emulator GUI communicationg with emulated payload, not using Digital Input/Output (DIO)

With the four DIOs turned off, the red light next to the corresponding wire on the DAQ is not illuminated, as seen in Figure 37.

Figure 37.    MCC DAQ controlled by C2B interface GUI, not using DIO

Figure 38 shows the GUI with the four DIOs, two for the C2B emulator and two for the payload.  This communication test was again successful, as the same text is shown in both GUI received file text box.  Figure 39 shows the DIOs being used, as were turned on using the GUI in Figure 38.

Figure 38.     C2B emulator GUI communicationg with emulated payload, using DIO
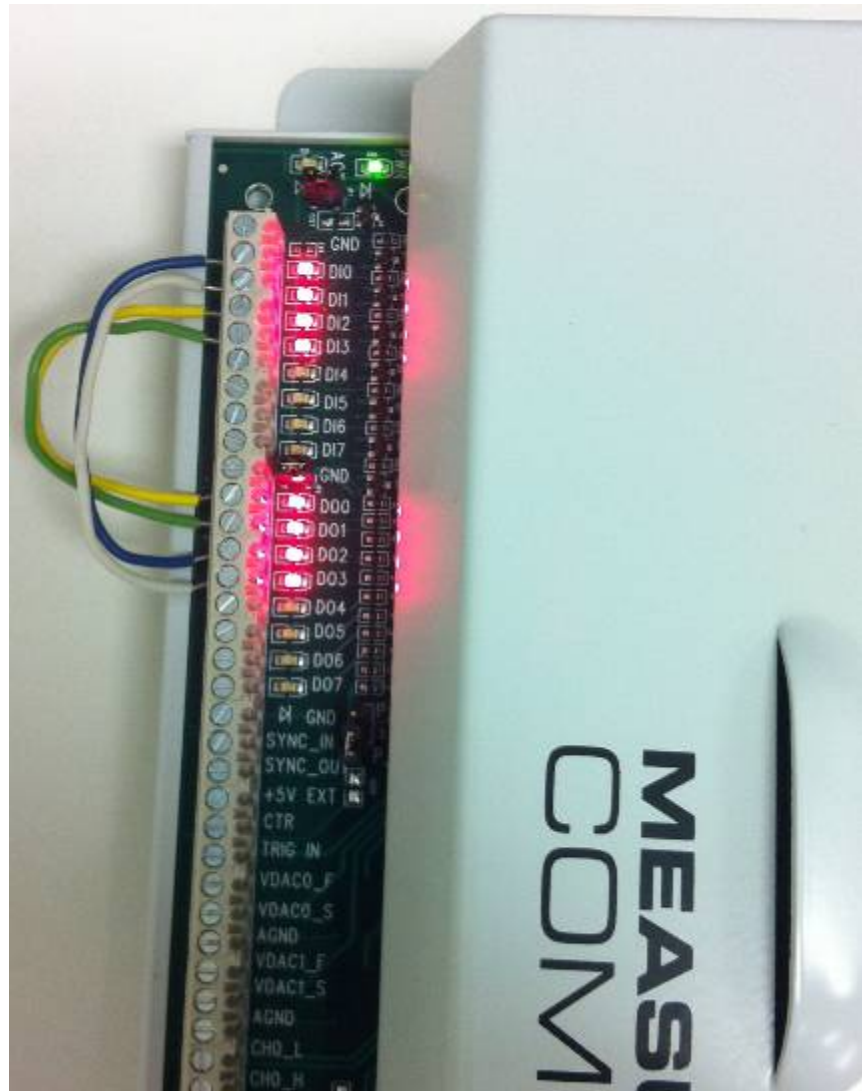
Figure 39.     MCC DAQ controlled by C2B interface GUI, using DIO

The GUI was created using the programming language Python.  Where Teraterm is useful for transferring human readable files, such as text or American Standard Code for Information Interchange (ASCII) characters, this GUI allows the binary formatted files.  Python required the use of a universal library to enable the GUI to communicate with the dynamic link layer (DLL) files of the DAQ, which is how the DIOs are controlled through the GUI.

THIS PAGE INTENTIONALLY LEFT BLANK

# IV. FUTURE INTEGRATION WORK

As this is the first thesis on this project, there is still much to do to prepare for the scheduled launch in May 2012, as seen in Table 3.

| Task | Date |
|------|------|
| Bus Emulator / Extender | Dec 2010 |
| C2B EDU Available | Jan 2011 |
| Integrated CAD Model Provided | Jan 2011 |
| C2B Flight Hardware Available | Feb 2011 |
| Payload EDU Certification | Jul 2011 |
| C2B / Payload Flight Unit Acceptance | Jul 2011 |
| Flight Unit Integration | Nov 2011 |
| End-to-End Flight Unit Test | Dec 2011 |
| Launch Opportunity | May 2012 |

Table 3.    Schedule for spacecraft completion and launch

## A.    COMPLETE C2B EMULATOR AND PAYLOAD EXTENDER

### 1.    C2B Emulator PCB

The C2B and payload integration requires the use of a PCB, as mentioned previously. To identify and correct potential problems, a prototype board, or proto-board, is first created to test some of the desired capabilities. Where the PCB uses the small connectors used in the actual spacecraft, the proto-board uses slightly larger holes and connectors, to ease making and testing connections. The proto-board will have the same digital signals and power inputs to the payload as the spacecraft, but in a more user-friendly format.

### 2. Payload Extender

Once the C2B emulator is complete, the payload extender will be utilized. The payload extender uses cables known as transfer cables. These transfer cables have both a male and a female end that extends the connector the length of the cable. Twelve inch cables are used to facilitate the extender. Since the payload extenders have been fitted to the C2B emulator, it will be tested again for signal strength to ensure the extender does not alter the signal level.

### B.   TEST C2B EMULATOR

Once the C2B emulator is complete, it must be tested. The signals coming from the DAQ digital input can be tested for continuity. The GUI will be used to facilitate the testing. More programming is also required for the C2B emulator to recognize particular message types and save the file to a specified location for that message type. For instance, if the payload sends the C2B binary formatted combined image data, the C2B must recognize what type of file is being received, and then store it in its corresponding location. Also, the C2B emulator must be programmed to capture and log data to a file. Sample data packets will be provided and used to transmit actual commands to the payload. Similarly, data packets will be sent from the payload to the C2B emulator to test its ability to recognize different types of files and save the data in the proper location.

Because the serial data connection already tested is the main source of communication between the bus and payload, the rest of the DIOs from the C2B are not used by the payload. Even though payload will not use the other C2B DIOs, the inputs will still be connected to create a higher fidelity C2B emulator, and allow flexibility in the additional tests that can be conducted.

### C.   COMPLETE AND TEST PAYLOAD EMULATOR

Just as the C2B emulator will aid in testing and integration, the payload emulator will provide the capability to overcome potential payload integration obstacles. By using another proto-board, the payload emulator will not be difficult to build. Having both a C2B emulator and a payload emulator enables the project to have an entire emulated

satellite on the workbench.  This greatly increases the testability and educational value. This allows NPS the ability to anticipate and eliminate any unforeseen difficulties. Additionally, with the C2B emulator, testing can be done on the payload.  Similarly, with the payload emulator, the spacecraft bus can be tested, as well as the communications between the bus and payload.

**D.      GROUND STATION PREPARATIONS**

The concept of operations has to be developed in order for NPS to operate the ground station for the satellite.  To accomplish, the list of commands, command names, and command descriptions needs to be provided by LLNL.  An example of the required concept of operations is the routine commands sent to the satellite, such as specific tasks to be completed at required intervals.

THIS PAGE INTENTIONALLY LEFT BLANK

# V.    CONCLUSION

This thesis chronicles the background, development, and initial steps to integrating an optical imager provided by Lawrence Livermore National Laboratories with a 3U CubeSat, the Boeing Colony II Bus, as part of the joint Space Situational Awareness project STARE with NPS and Texas A&M University.  The imager captures time-lapse streaks of other satellites.  Analyzing these streaks will provide data to improve the orbital ephemeris of the imaged satellite.

Work done in support of STARE includes performing STK analysis proving the project's feasibility, developing the PCB and penta-harness for integrating the C2B and payload, making the decision to move forward with the PCB instead of the penta-harness, creating the communications link, including the active component level shifter, between the bus and payload, and programming a GUI to communicate with the DAQ in order to use specific DIOs, emulating the C2B.  Future work includes completing and testing the C2B emulator, laying out the integration PCB, and developing the ground station concept of operations.

THIS PAGE INTENTIONALLY LEFT BLANK

# LIST OF REFERENCES

[1]     P. Bournes. "CubeSat Experiments," presented at CubeSat Workshop, San Luis Obispo, CA, 2009.

[2]     Space Situational Awareness Factsheet: Promoting Cooperative Solutions for Space Security, June 2008. <http://www.secureworldfoundation.com>.

[3]     Space Based Space Surveillance, Global Security. <http://www.globalsecurity.org/space/systems/sbss.htm>.

[4]     United Nations Office for Outer Space Affairs, "Space Debris Mitigation Guidelines of the Committee on the Peaceful Uses of Outer Space," Vienna, 2010.

[5]     J. Foust, "The Chinese ASAT Enigma," The Space review: Essays and Commentary about the Final Frontier., May 2007.

[6]     Center for Space Standards and Innovation, Chinese ASAT Test. <http://www.centerforspace.com/asat/>.

[7]     G. Forden, "A Preliminary Analysis of the Proposed USA-193 Shoot-down." Feb. 2008.

[8]     Space Primer, Chapter 21, Space Surveillance Theory and Network.

[9]     G. Stokes, C. Braun, R. Sridharan, D. Harrison, J. Sharma, "The Space-Based Visible Program," Lincoln Laboratory Journal, vol. 11, No. 2, 1998.

[10]    Air University, Maxwell AFB, AL, "Space Surveillance Theory and Network," Air University Space Primer, August, 2003, Chapter 21.

[11]    Space Based Space Surveillance: Enhancing the Nation's Space Situational Awareness, 2009.

[12]    STK help. < http://www.stk.com/resources/help/online/stk/source/stk/constraints-02.htm>.

[13]    R. Abbot and T. Wallace, "Decision Support in Space Situational Awareness," Lincoln Laboratory Journal, vol. 15, no. 2, Nov. 2007.

[14]    J. Wertz and W. Larson, Space Mission Analysis and Design. Hawthorne, CA: Microcosm Press, 2008.

[15]     C. Day, "Advanced CubeSat Avionics—A Next Generation Approach for Highly Capable and Integrated Vehicles," presented at CubeSat Workshop, San Luis Obispo, CA, 2010.

[16]     B. Iannotta nd T. Maliq, "U.S. Satellite Destroyed in Space Collision," Space News, Feb. 2009.

[17]     FFSD, FFMD Series Information Sheet, Samtec <www.samtec.com>.

[18]     Launch of Cosmos-2428, the Last Tselina-2 Electronic Intelligence Satellite, June 2007.
         <http://russianforces.org/blog/2007/06/launch_of_cosmos2428_the_last.shtml>

[19]     Dot Product, Wikipedia. <http://en.wikipedia.org/wiki/Dot_product>

[20]     SMT Micro Header Information sheet, Samtec <www.samtec.com>

# INITIAL DISTRIBUTION LIST

1. Defense Technical Information Center
   Ft. Belvoir, Virginia

2. Dudley Knox Library
   Naval Postgraduate School
   Monterey, California

3. Professor James Newman
   Naval Postgraduate School
   Monterey, California

4. Professor Marcello Romano
   Naval Postgraduate School
   Monterey, California